

Research Article

Modeling the Impact of Virtual Contact Network with Community Structure on the Epidemic Spreading

Jianlin Zhou  and Haiyan Liu 

School of Economics and Management, China University of Geosciences (Beijing), Beijing 100083, China

Correspondence should be addressed to Haiyan Liu; liuhy@cugb.edu.cn

Received 21 June 2021; Revised 8 December 2021; Accepted 29 December 2021; Published 21 January 2022

Academic Editor: Hocine Cherifi

Copyright © 2022 Jianlin Zhou and Haiyan Liu. This is an open access article distributed under the Creative Commons Attribution License, which permits unrestricted use, distribution, and reproduction in any medium, provided the original work is properly cited.

The epidemic spreading is closely related to the spread of information, and it will coevolve with the information transmission. Considering that the network structure has a significant impact on network dynamics and the virtual contact networks have obvious community structures in reality, in this article, we built a multiplex network, which contains a community structure to explore the interplay of the coupled spread dynamics. We first use a microscopic Markov chain approach to characterize the coupled disease-awareness dynamics and then analyze the effect of different factors on the coevolution of information dissemination and epidemic spreading based on the Monte Carlo simulation. The simulation results show that promoting the dissemination of information is indeed conducive to suppressing the spread of disease, but changing the process of disease transmission has no obvious effect on the information dissemination. The analysis also reveals that increasing the information transmission rate or decreasing the information recovery rate can promote the spread of information and inhibit the spread of diseases. In addition, taking preventive behaviors or decreasing the long-distance jump also helps slow the epidemic spreading.

1. Introduction

Every outbreak of infectious diseases will cause immeasurable losses, especially, the outbreak of coronavirus disease 2019 (COVID-19); as of May 15, 2021, it has infected more than 160 million people and has caused more than 3.3 million deaths worldwide. In order to control the spread of the disease, it is important to understand the mechanism and influencing factors of the epidemic spreading. The spread of disease is not an independent process, and it is closely related to information dissemination about the disease and human preventive behavior [1–3]. For instance, when information about the disease spreads through various communication platforms, individuals who are aware of this information will take certain preventive actions, such as wearing masks, washing hands, and maintaining physical distancing, to protect themselves. These preventive behaviors can affect the dynamics of disease transmission and suppress the outbreak of the epidemic. At present, exploring the interaction between information transmission and disease transmission has become a novel research topic [4–7].

Compartmental models, such as susceptible-infected-susceptible (SIS) model, susceptible-infectious-recovered (SIR) model, and susceptible-exposed-infected-recovered (SEIR) model, are originally used to describe the dynamics of disease transmission [8]. But these traditional models need to assume that the population is homogeneous and well mixed. With the rapid development of network science, complex network models of epidemics break the above limitations and provide a new perspective for exploring the dynamics of disease transmission [9]. These complex network models can represent heterogeneous population structure and interaction patterns among individuals to a certain extent. Researchers have explored various dynamic processes of disease transmission on different types of complex networks (e.g., random networks, small-world networks, scale-free networks, weighted networks, adaptive networks) [10–15]. Most previous studies only focus on the epidemic spreading and do not consider more other dynamic processes. At present, some studies have explored the coevolution of awareness and epidemics on single and multiplex networks, where the information about the disease

is called awareness [3]. For the coevolution of awareness and epidemic on single networks, Funk et al. link the information dissemination model with an epidemiological SIR model to study how the spread of awareness affects the spread of a disease [4]. They find that spreading the awareness of the disease can result in a lower epidemic size. On the basis of this study, Funk et al. then overlay the SIS model of information dissemination with the epidemiological susceptible-infected-recovered-susceptible (SIRS) model to study the interaction between local behavioral response and endemic disease [16]. Ruan et al. link the epidemiological SIR model with the information dissemination model to study the coevolution of the crisis awareness and epidemic spreading [17]. They find that the epidemic spreading can be suppressed when the information creation rate and the sensitivity to information are large.

Disease transmission usually takes place in the physical contact networks, and information dissemination takes place in the virtual contact networks, which can be built through different communication platforms, such as phone calls, Facebook, Twitter, and WeChat. The structure of physical contact networks and virtual contact networks is usually very different. Therefore, it is inappropriate to simulate the coevolution of awareness and epidemics on a single network. Some scientists have paid attention to this issue and they use multiplex networks to simulate the spread of diseases and information [18–29]. For instance, Granell et al. study the interplay between awareness and epidemic spreading based on a multiplex network, which contains two layers: the virtual contact layer and the physical contact layer [18]. They use the unaware-aware-unaware (UAU) model to describe the process of disease transmission, which takes place in the virtual contact layer and uses the SIS model in the physical layer to simulate the epidemic spreading. They find that the onset of the epidemics has a critical value. Many previous studies assume that the time scale of multiplex network evolution is much longer than the spreading dynamics; therefore, multiplex networks are often regarded as static networks [3]. But in reality, individuals may move at any time, so the physical contact work is a dynamic network. Some studies have explored the dynamical interaction between disease transmission and information dissemination by constructing dynamic multiplex networks [30, 31]. For example, Xia et al. construct a double-layer network to explore the coevolution of information and epidemic spreading, where the top layer is a static communication network and the bottom layer is a dynamical physical contact network [30]. Yang et al. construct an epidemic spread-information dissemination coupling network considering the movements of individuals across regions to analyze the dynamic evolution of the spreading process [31]. In addition, many studies have shown that the topology of the network can significantly affect the dynamics of disease transmission [32, 33]. Previous studies assume that the virtual contact network is a power-law degree distribution network and analyze the impact of this network structure on disease and information dissemination. In reality, virtual contact networks often contain community structures, which has a significant impact on the spread of information

[34]. Therefore, when investigating the coevolution of information and disease, the virtual contact network with community structure should not be ignored.

Considering the influence of community structure on information dissemination, in this article, we first build a multiplex virtual-physical network, where the virtual contact network has a community structure and the physical contact network is a dynamic network. We then use an unaware-aware-recovered + susceptible-infected-recovered (UAR + SIR) model on this multiplex network to reveal the interplay between information and disease spreading. We perform Monte Carlo (MC) simulation to show the coevolution of information and epidemic spreading and investigate the effect of different factors on the spreading dynamics. The results show that the increasing information transmission rate or the probability of taking preventive behaviors and decreasing the long-distance jump probability or information recovery rate can reduce the scope of disease transmission. We also find that the dynamic of information dissemination is only sensitive to the information transmission rate and the information recovery rate, and it is not sensitive to other model parameters.

2. Model

2.1. Multiplex Virtual-Physical Contact Network. To understand the interplay between information and epidemic spreading process, we simulate these two processes in a multiplex network. This multiplex network consists of two layers. The top layer is a communication network with a community structure, and the bottom layer is a physical contact network with moving agents and regional structure presented in Figure 1(a). The top layer can be called the virtual layer, and the information is diffused upon this layer through virtual contact between individuals. The bottom layer can be called the physical layer, and the diffusion of infectious diseases takes place in this layer through physical contact between individuals.

The communication network is an undirected graph, where nodes represent individuals and links represent their relationships of information transmission. In the real world, communication networks often display a community structure, where the contacts between individuals in the same community are more frequent, whereas the contacts between individuals in different communities are relatively few. In order to make our model closer to the characteristics of the empirical communication networks, we make the communication network in the virtual layer also have a community structure. In addition, since the contacts between individuals in a short period of time is relatively stable, we assume that the links in the communication network will remain unchanged in the short term. That is to say, the communication network in the virtual layer is a static network in the short term.

The physical contact network is also an undirected network, where nodes are individuals and the link between two nodes indicates that these two individuals are interacting within a certain radius. Since each individual can

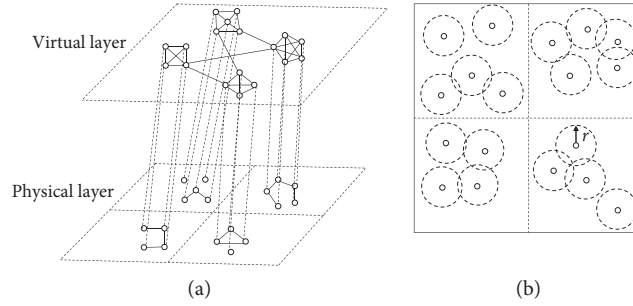


FIGURE 1: Illustration of multiplex virtual-physical contact network. (a) Virtual contact network with community structure and dynamic physical contact network. (b) Individuals perform random walk in a planar space.

move, the link between the two individuals in the physical contact network may disappear at the next moment. Therefore, the structure of the physical contact network changes dynamically over time. Based on the existing dynamical network model [35–37], we assume that the physical contact network contains N individuals and these moving individuals are distributed in a planar space $\Gamma = \{(x, y) \in \mathbb{R}^2: 0 \leq x \leq L, 0 \leq y \leq L\}$. Individuals are represented as point particles. In particular, we consider that people in real life tend to move within fixed areas and rarely move across areas. In order to simulate this phenomenon in the model, we divide the planar space Γ into four equal parts and in the initial state N , individuals are uniformly distributed in these places shown in Figure 1(b). The position of i -th individual in the planar space at time t is denoted as $\mathbf{P}_i(t) = (x_i(t), y_i(t))$, and its velocity $\mathbf{V}_i(t) = (v_i(t) \cos \theta_i(t), v_i(t) \sin \theta_i(t))$, $i = 1, 2, \dots, N$. We assume that the individual's moving speed is a constant in time and each individual has the same speed, that is, $v_i(t) = v$, $\forall i = 1, 2, \dots, N$ and $\forall t$. At each time step, the i -th individual will stochastically change the moving direction angles $\theta_i(t)$. Then, the positions and the orientations of node i at time $t + 1$ are updated based on the following rule:

$$\begin{aligned} x_i(t+1) &= x_i(t) + v_i(t) \cos \theta_i(t), \\ y_i(t+1) &= y_i(t) + v_i(t) \sin \theta_i(t), \\ \theta_i(t+1) &= \xi_i(t+1), \end{aligned} \quad (1)$$

where $\xi_i(t+1)$ is a random variable and it is chosen from a uniform probability distribution in the interval $[-\pi, \pi]$. In addition, we assume that each individual has its own interaction radius and the interaction radius of the i -th individual is denoted by r_i . In this article, we assume that all individuals have equal interaction radius r . Then, the distance between two nodes i and j in the physical layer at time t can be measured by the Euclidean distance, and it is defined as

$$d_{ij}(t) = \sqrt{(x_i(t) - x_j(t))^2 + (y_i(t) - y_j(t))^2}, \quad i, j = 1, 2, \dots, N. \quad (2)$$

When we know the distance between any two nodes in the physical layer and their radius, we can build a physical contact network. For any two nodes i and j in the physical layer, if their distance $d_{ij}(t) \leq r$, an edge will be established between

node i and node j . In addition, considering that the individual can travel with time scales much shorter than those related to epidemic dynamics such as traveling by flights, we allow individuals to perform long-distance jumps in the physical layer. The probability of an individual making a long-distance jump is denoted by $p_{\text{jump}} \in [0, 1]$, which quantifies the probability of an individual jumping from the current region to other regions. To sum up, at each time step, any individual in the physical layer can have two choices: it moves either following (1) with probability $1 - p_{\text{jump}}$ or performing a long-distance jump from the current region to another region with probability p_{jump} . After the individuals have moved, we then compare the distance between individuals with interaction radius and establish the edges between nodes. So at each time step, we can obtain a physical contact network.

2.2. Diffusion of Information and Disease. The spread of disease takes place on the physical layer, and we use the classic SIR model to simulate the epidemic spreading. The SIR model divides N individuals into three disjoint groups: susceptible (S), infected (I), and recovered (R). The individuals in state S have not contracted the disease, but they can be infected. The individuals in state I have contracted the disease, and they can transmit the disease to the susceptible individuals. Besides, the infected individuals can also recover after treatment. Once the individuals are in the recovery state, they will no longer be infected or spread disease. We define $S(t)$, $I(t)$, $R(t)$ as the fractions of susceptible, infected, and recovered individuals at time t , where $S(t) + I(t) + R(t) = 1$. We assume that when a susceptible individual comes into contact with an infected individual, its state becomes state I with probability β_1 and maintains the original state with probability $1 - \beta_1$. We call the probability β_1 the disease transmission rate. For each infected individual, at each time step, their state can become recovered state with probability γ_1 and stay in the infected state with probability $1 - \gamma_1$. The probability γ_1 is called disease recovery rate. When we simulate the spread of disease in the physical contact network, at the initial time $t = 0$, some nodes will be randomly selected as infected nodes and all other nodes are in a susceptible state. After that, the nodes in the infected state will infect its neighbors at each step, the number of nodes in the susceptible state will decrease, while the number of nodes in the recovered state will increase.

We simulate the spread of information in the virtual layer, and this diffusion process is also modeled based on the SIR model. The N individuals in the virtual network are also divided into three groups: unaware (U), aware (A), and recovered (R). When an epidemic breaks out, the individuals in state U do not have the information about the disease. The individuals in state A know the information about the disease and pass it to other people with a certain probability. The individuals in state R also receive the information about the disease, but they do not want to tell other people. For an unaware individual, there are two paths to transform from state U to state A : either the communication with neighbors in state A or the individual is already sick (i.e., the individual at the physical layer is in state I). When an unaware individual contacts an aware individual, we assume that its state becomes state A with probability β_2 and maintains the original state with probability $1 - \beta_2$. For each aware individual, at each time step, their state can become recovered state with probability γ_2 and stay in the aware state with probability $1 - \gamma_2$. We call the probability β_2 and probability γ_2 the information transmission rate and information recovery rate. In addition, we also assume that when a healthy individual is aware of the information about the epidemic, the individual will take preventive actions with the probability p_{prevent} . These preventive behaviors can reduce the probability of being infected and make the disease transmission rate with a probability $(1 - \omega)\beta_1$. The parameter ω represents the effect of taking protective actions on disease prevention. In all simulation experiments, we fix $\gamma_1 = 0.2$ and $\gamma_2 = 0.2$. Therefore, the effective disease transmission rate can be defined as $\beta_1/0.2$, and the effective information transmission rate can be defined as $\beta_2/0.2$.

The virtual contact network and the physical contact network can be described by the adjacency matrices $(a_{ij})_{N \times N}$ and $(b_{ij})_{N \times N}$, respectively, where $a_{ij} = 1$ represents there is virtual contact between node i and node j and $a_{ij} = 0$ otherwise, and $b_{ij} = 1$ indicates there is physical contact between node i and node j and $b_{ij} = 0$ otherwise. It needs to

be pointed out that the adjacency matrix $(b_{ij})_{N \times N}$ changes dynamically over time, because the physical contact network is a dynamic network. Then, we use the microscopic Markov chain approach (MMCA) to describe the coevolution of disease transmission and information transmission. During the spread of information and disease, an individual can have seven possible states: unaware and susceptible (US), aware and susceptible (AS), aware and infected (AI), aware and recovered (AR_p), recovered and susceptible ($R_V S$), recovered and infected ($R_V I$), and recovered and recovered ($R_V R_p$), where R_V and R_p represent the individual is in a state of recovery at the virtual layer or physical layer, respectively. The probability of node i being in one of the above states at time t is denoted by $p_i^{\text{US}}(t)$, $p_i^{\text{AS}}(t)$, $p_i^{\text{AI}}(t)$, $p_i^{\text{AR}_p}(t)$, $p_i^{\text{R}_V S}(t)$, $p_i^{\text{R}_V I}(t)$, and $p_i^{\text{R}_V R_p}(t)$. We assume that the probability of node i in state U not being informed by any neighbors is $\theta_i(t)$, the probability of node i not being infected by any neighbors if node i is aware of the information of disease is $q_i^A(t)$, and the probability of node i not being infected by any neighbors if node i is in the unaware state is $q_i^U(t)$. The above probabilities are described as follows:

$$\begin{aligned} \theta_i(t) &= \prod_j [1 - a_{ji} p_j^A(t) \beta_2], \\ q_i^A(t) &= p_{\text{prevent}} \prod_j [1 - b_{ji} p_j^I(t) 0.4 \beta_1] \\ &\quad + (1 - p_{\text{prevent}}) \prod_j [1 - b_{ji} p_j^I(t) \beta_1], \\ q_i^U(t) &= \prod_j [1 - b_{ji} p_j^I(t) \beta_1], \end{aligned} \quad (3)$$

where $p_j^A(t) = p_j^{\text{AS}}(t) + p_j^{\text{AI}}(t) + p_j^{\text{AR}_p}(t)$ and $p_j^I(t) = p_j^{\text{AI}}(t) + p_j^{\text{R}_V I}(t)$. Based on the transition probability trees presented in Figure 2, the MMCA equations of the coevolution dynamic for each node i are as follows:

$$\begin{aligned} p_i^{\text{US}}(t+1) &= p_i^{\text{US}}(t) \theta_i(t) q_i^U(t), \\ p_i^{\text{AS}}(t+1) &= p_i^{\text{US}}(t) (1 - \theta_i(t)) q_i^A(t) + p_i^{\text{AS}}(t) (1 - \gamma_2) q_i^A(t), \\ p_i^{\text{AI}}(t+1) &= p_i^{\text{US}}(t) \theta_i(t) (1 - q_i^U(t)) + p_i^{\text{AS}}(t) (1 - \theta_i(t)) (1 - q_i^A(t)) \\ &\quad + p_i^{\text{AS}}(t) (1 - \gamma_2) (1 - q_i^A(t)) + p_i^{\text{AI}}(t) (1 - \gamma_2) (1 - \gamma_1), \\ p_i^{\text{AR}_p}(t+1) &= p_i^{\text{AI}}(t) (1 - \gamma_2) \gamma_1 + p_i^{\text{AR}_p}(t) (1 - \gamma_2), \\ p_i^{\text{R}_V S}(t+1) &= p_i^{\text{AS}}(t) \gamma_2 q_i^A(t) + p_i^{\text{R}_V S}(t) q_i^A(t), \\ p_i^{\text{R}_V I}(t+1) &= (p_i^{\text{AS}}(t) \gamma_2 + p_i^{\text{R}_V S}(t)) (1 - q_i^A(t)) + (p_i^{\text{AI}}(t) \gamma_2 + p_i^{\text{R}_V I}(t)) (1 - \gamma_1), \\ p_i^{\text{R}_V R_p}(t+1) &= p_i^{\text{AI}}(t) \gamma_2 \gamma_1 + p_i^{\text{AR}_p}(t) \gamma_2 + p_i^{\text{R}_V I}(t) \gamma_1 + p_i^{\text{R}_V R_p}(t). \end{aligned} \quad (4)$$

When the coevolution dynamic reaches the stationary state, we can obtain $p_i^{\text{US}}(t+1) = p_i^{\text{US}}(t) = p_i^{\text{US}}$ and, equivalently, for other states.

3. Results

Before simulating the spread of disease and information, we first construct the virtual-physical contact network. Considering that the virtual contact network has a community

structure, we adopt the artificial benchmark [38] designed by Girvan and Newman to build a virtual contact network with 1000 nodes. These nodes are assigned to four communities with different nodes each: 50, 150, 300, and 500 nodes. The link density within a community and the link density between communities are tuned by two parameters p_{in} and p_{out} , respectively. If two nodes belong to the same community, they are connected with probability p_{in} ; if two nodes belong to different communities, they are connected with

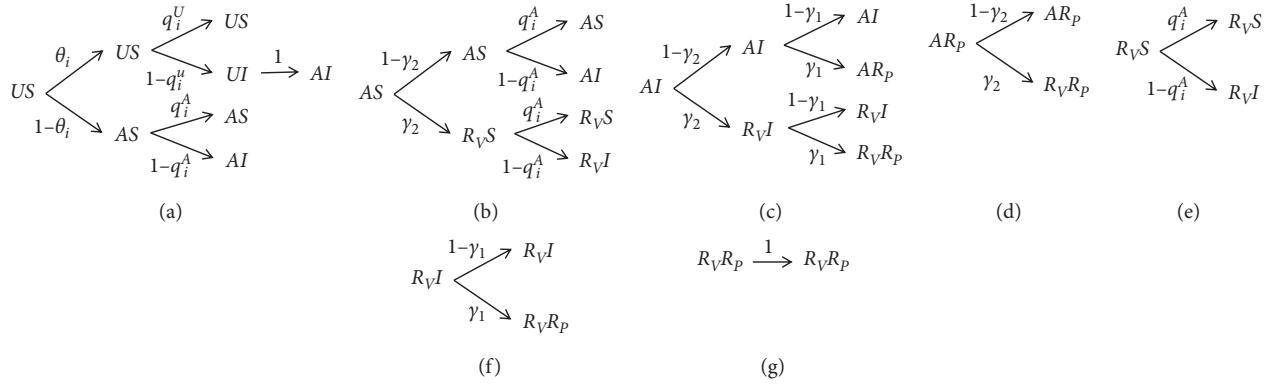


FIGURE 2: Transition probability trees for the seven possible states in the UAR-SIR model.

probability p_{out} . By setting these two parameters and the number of nodes, we can get a static virtual contact network. In this article, the two parameters p_{in} and p_{out} are set to 0.0193 and 0.0016, respectively, which makes the expected degree of each node equal to 6. The nodes in the virtual contact network correspond to the nodes in the physical contact network. To construct a physical contact network, we simulate the movement of individuals on a planar space. The width of the planar space L is set to $\sqrt{1000}$, which makes the density of individuals in the plane space equal to 1. This flat space is equally divided into four areas, and the width of each area is equal to $L/2$. The individual's moving speed v is set to 0.03, and the interaction radius of each individual is set to 1. At the initial time $t = 0$, nodes belonging to the same community in the virtual contact network are randomly placed in the same area in the plane space. As long as the distance between two nodes in the plane space is less than the interaction radius r , an edge is added between these two nodes and, finally, we can get the physical contact network. Since nodes move at each time step, the physical contact relationship between nodes will change. Therefore, the physical contact network is a dynamic network and its network structure changes over time. When the virtual-physical contact network has been built, we simulate the spread of information and disease on this network. Then, we will analyze the factors that influence the interaction between information and disease. In addition, we generate the virtual contact networks without community structure by randomly rewiring the above virtual contact networks. In this article, we compare the coupled spread dynamics in the two scenarios—virtual contact networks with or without community structure.

Before the simulations with different initial conditions start, we assume that there are 2% of infected nodes in each area. Then, the disease and information follow the SIR dynamic model to spread. The entire spreading process will end until there are no more infected nodes and aware nodes in the virtual-physical contact network. All simulation results below are averaged over 30 experiments. Firstly, in Figure 3, we give a case to show the evolution process of information diffusion and disease diffusion. The relevant parameters are set as follows: $\beta_1 = 0.2$, $\beta_2 = 0.3$, $p_{\text{prevent}} = 0.8$, $\omega = 0.6$, $p_{\text{jump}} = 0.2$. Figure 3(a) shows the evolution of the density of nodes with

different states in the physical layer. One can find that the density of susceptible individuals gradually decreases with time and then reaches the steady state. The density of infected individuals first increases rapidly to reach a peak and then gradually decreases to zero over time. The density of recovered individuals gradually increases over time and then reaches the steady state. We observe that the density of individuals in different states can reach a steady state after about 80 steps and finally the density of recovered individuals is greater than the density of susceptible individuals. The evolution of the density of nodes with different states in the virtual layer is shown in Figure 3(b). We can observe that the density of unaware individuals drops rapidly and then reaches a steady state. The density of aware individuals first increases rapidly, then decreases rapidly, and finally gradually decreases to zero. The density of recovered individuals in the virtual layer increases rapidly with time and then gradually reaches a steady state. The final density of recovered individuals is much greater than the final density of unaware individuals. In addition, compared with the process of epidemic spreading, we can see that information dissemination can reach a steady state faster.

The classic SIR model contains multiple parameters such as transmission rate and recovery rate. These parameters will affect the spread of disease or information. Then, we investigate how the parameters in our model affect information and disease transmission. We first explore the impact of epidemic transmission rate β_1 on disease and information dissemination. The result is shown in Figure 4, and we fix some parameters: $\beta_2 = 0.3$, $p_{\text{prevent}} = 0.8$, $p_{\text{jump}} = 0.2$, and $\omega = 0.6$ and consider different epidemic transmission rates: $\beta_1 = 0.1, 0.3, 0.5$. In Figures 4(a) and 4(b), we observe that the peak value of the density of the infected nodes and the final density of recovered nodes in the physical layer increase obviously as the parameter β_1 becomes larger. Besides, when the parameter β_1 changes from 0.1 to 0.3, the final density of recovered nodes in the physical layer changes greatly compared to the parameter β_1 from 0.3 to 0.5. In Figures 4(c) and 4(d), although we can see that the aware population and recovered population in the virtual layer also increase as β_1 becomes larger, this increase is not very obvious. The simulation results indicate that the disease transmission process is more sensitive to the parameter β_1 than the

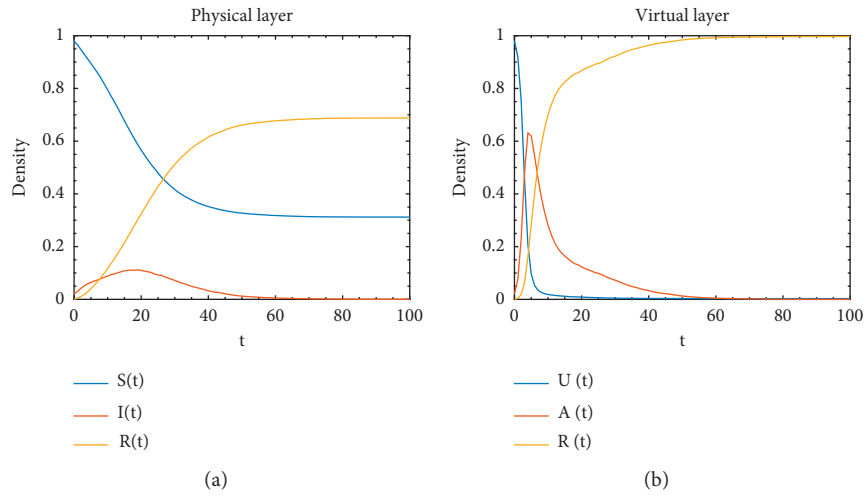


FIGURE 3: Temporal progress of epidemic spreading and information dissemination. (a) The evolution of epidemic spreading over time. (b) The evolution of information dissemination over time.

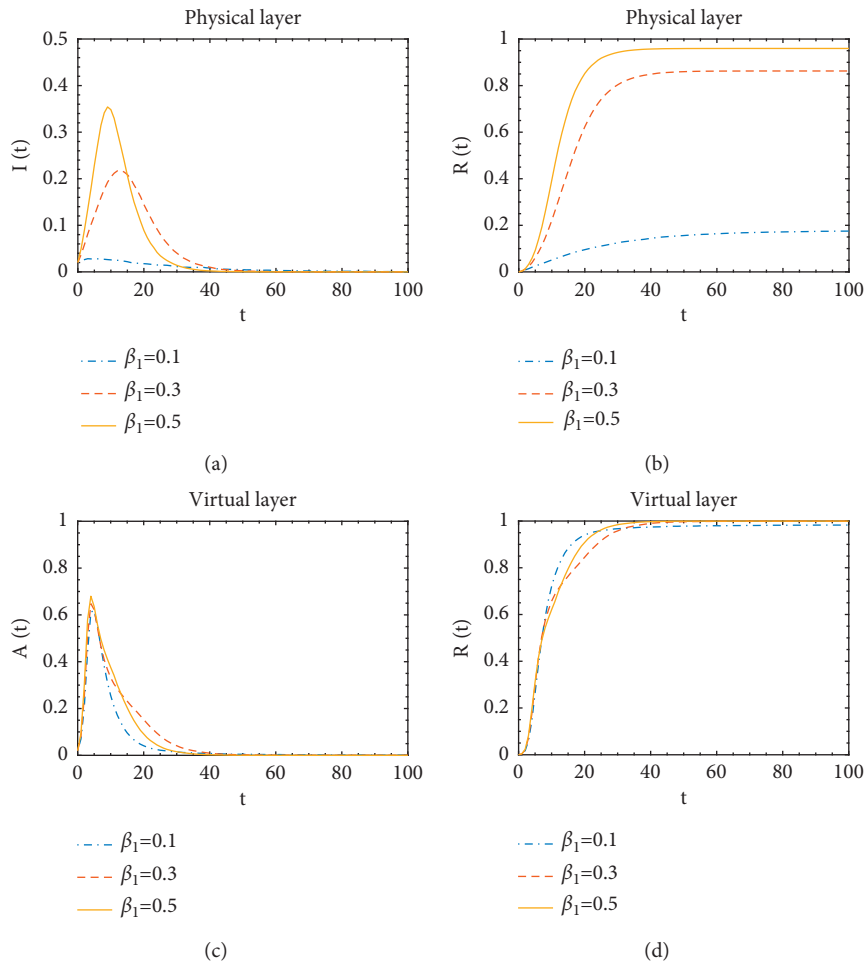


FIGURE 4: Continued.

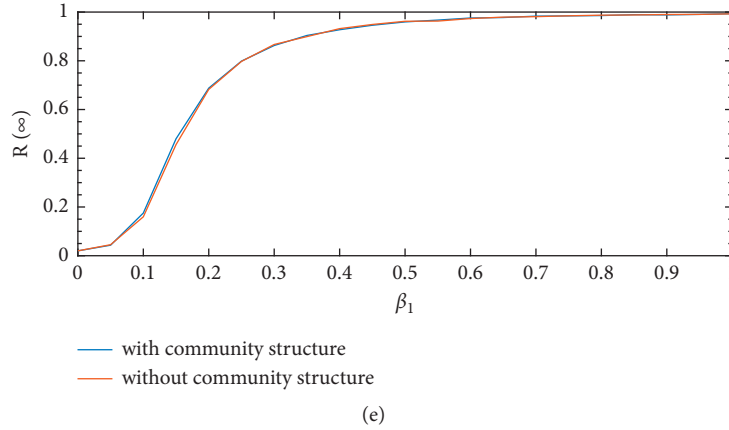


FIGURE 4: The influence of epidemic transmission rate on the coupled disease-awareness model. (a) Density of infected individuals in the physical layer as a function of time. (b) Density of recovered individuals in the physical layer as a function of time. (c) Density of aware individuals in the virtual layer as a function of time. (d) Density of recovered individuals in the virtual layer as a function of time. (e) The final density of recovered individuals in the physical layer under different disease transmission rates for the virtual contact networks with or without community structure.

information dissemination. Figure 4(e) shows the final density of recovered individuals in the physical layer under different disease transmission rates. When $0.1 \leq \beta_1 \leq 0.2$, the final density of the recovered individuals is growing rapidly with parameter β_1 . When $\beta_1 > 0.5$, the final density of the recovered individuals remains stable and it is close to 1. We also find that the community structure of virtual contact network does not significantly affect the spread of disease.

To explore whether there is a disease transmission threshold, we observe the changes in the density of infected individuals in the physical layer over time under different disease transmission rate. We fix some parameters: $\beta_2 = 0.3$, $p_{\text{prevent}} = 0.8$, $p_{\text{jump}} = 0.2$, $\omega = 0.6$. The result is shown in Figure 5. We can find that when the parameter β_1 is greater than 0.1, the peak values of the density of the infected nodes are increasing as the parameter β_1 becomes larger. But when the parameter β_1 is less than 0.1, the density of the infected nodes in the physical layer decreases with time and approaches 0. So the threshold for disease transmission is between 0.1 and 0.15.

Next, in Figure 6, we investigate the influence of the information transmission rate β_2 on information dissemination and disease transmission. In Figure 6, the fixed parameters are as follows: $\beta_1 = 0.2$, $p_{\text{prevent}} = 0.8$, $p_{\text{jump}} = 0.2$, $\omega = 0.6$. When the value of the parameter β_2 is increased, it makes the aware people pass the epidemic information to others with a greater probability. At this time, more unaware individuals are converted to aware individuals and they will take defensive actions to slow the epidemic spreading. As shown in Figures 6(a) and 6(b), with the increase in information transmission rate β_2 , the peak value of the density of infected individuals decreases and the final density of recovered individuals will be slightly smaller. This indicates that increasing the information dissemination rate β_2 can slow down the spread of diseases to a certain extent. The increase of parameter β_2 significantly accelerates the information dissemination

shown in Figures 6(c) and 6(d). It can be clearly observed that as the parameter β_2 changes from 0.1 to 0.5, the peak value of the density of aware individuals increases obviously. The final density of recovered individuals in the virtual layer also increases. In addition, in Figure 6(e), we also explore the final density of the recovered individuals in the physical layer under different information transmission rate β_2 . We can observe that the increase in the rate of information dissemination can indeed curb the spread of diseases. But when the parameter β_2 is greater than 0.2, the increase of β_2 will no longer reduce the final density of recovered individuals in the virtual layer.

If susceptible individual adopts protective behaviors, it will reduce the probability of turning him or her into an infected individual. Then, we explore the impact of the probability of individuals taking preventive behaviors p_{prevent} on disease and information dissemination, and the results are shown in Figure 7. The fixed parameters are as follows: $\beta_1 = 0.2$, $\beta_2 = 0.3$, $p_{\text{jump}} = 0.2$, $\omega = 0.6$. In Figures 7(a) and 7(b), we can observe that the peak value of the density of infected individuals and the final density of recovered individuals decrease as the parameter p_{prevent} increases. When the parameter p_{prevent} increases from 0.4 to 0.8, the peak value of the density of infected individuals decreases. Compared with Figures 7(a) and 7(b), it can also be clearly seen that parameter p_{prevent} has a greater impact on disease transmission than parameter β_2 . However, increasing the probability of taking preventive behavior has little impact on information dissemination shown in Figures 7(c) and 7(d). We can see that the density evolution curves of aware and recovered individuals in the virtual layer under different p_{prevent} are basically similar. We also investigate the final density of the recovered individuals in the physical layer under different parameters p_{prevent} , and the result is shown in Figure 7(e). We find that the final density of recovered individuals in the physical layer decreases with the increase of probability p_{prevent} .

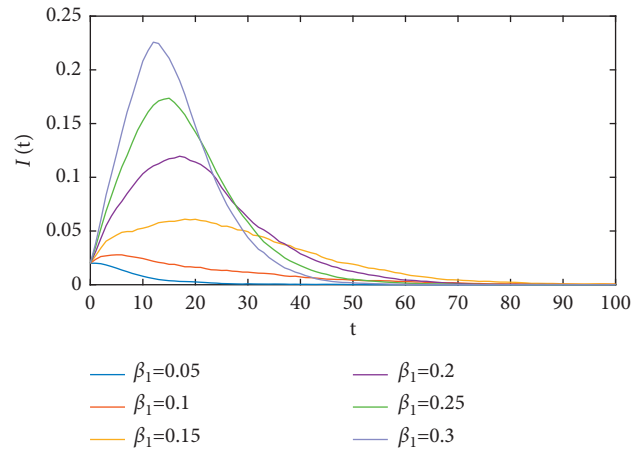


FIGURE 5: The density of infected individuals in the physical layer as a function of time for different epidemic transmission rates.

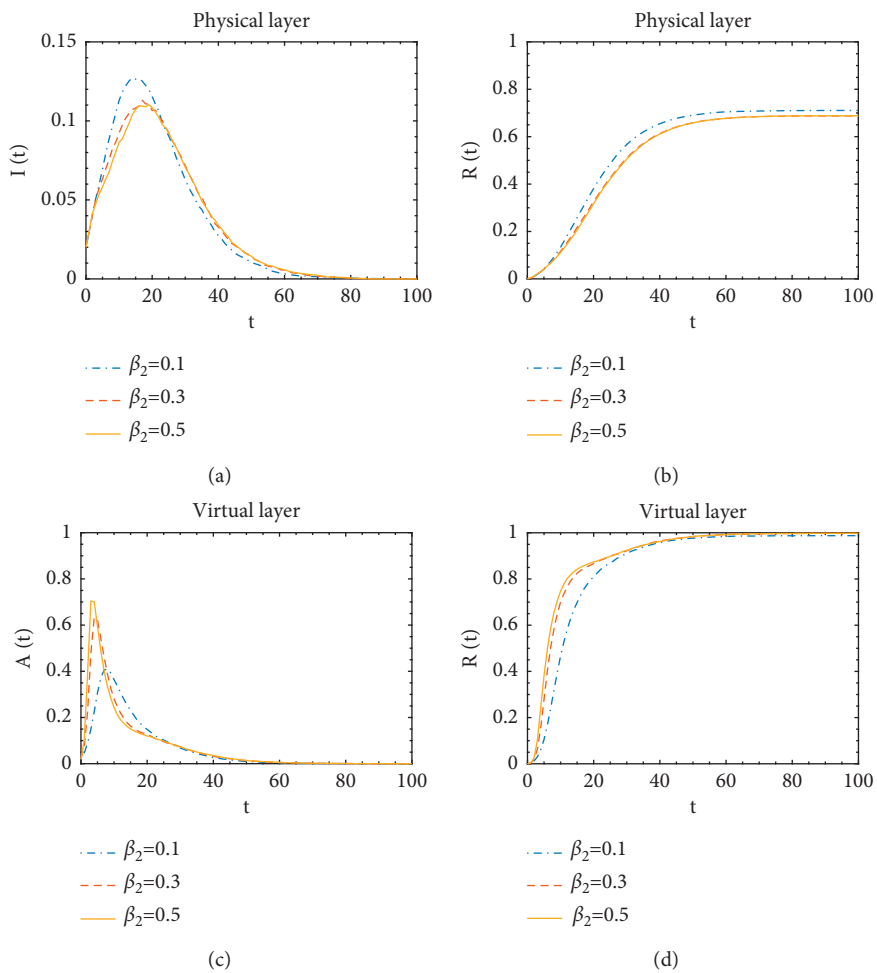


FIGURE 6: Continued.

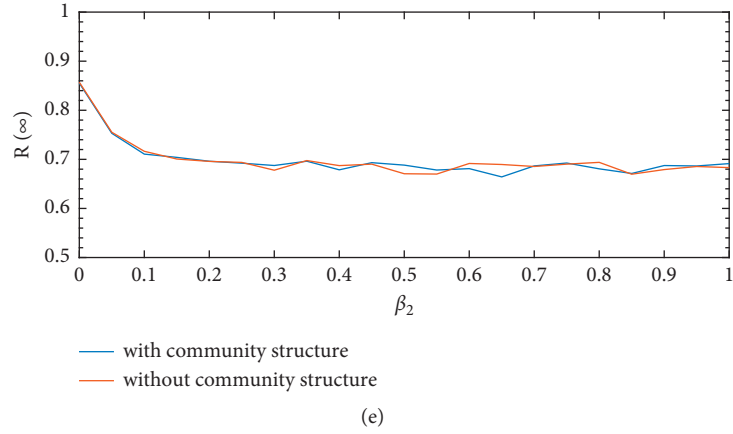


FIGURE 6: The influence of information transmission rate on the coupled disease-awareness model. (a) Density of infected individuals in the physical layer as a function of time. (b) Density of recovered individuals in the physical layer as a function of time. (c) Density of aware individuals in the virtual layer as a function of time. (d) Density of recovered individuals in the virtual layer as a function of time. (e) The final density of recovered individuals in the physical layer under different information transmission rates for the virtual contact networks with or without community structure.

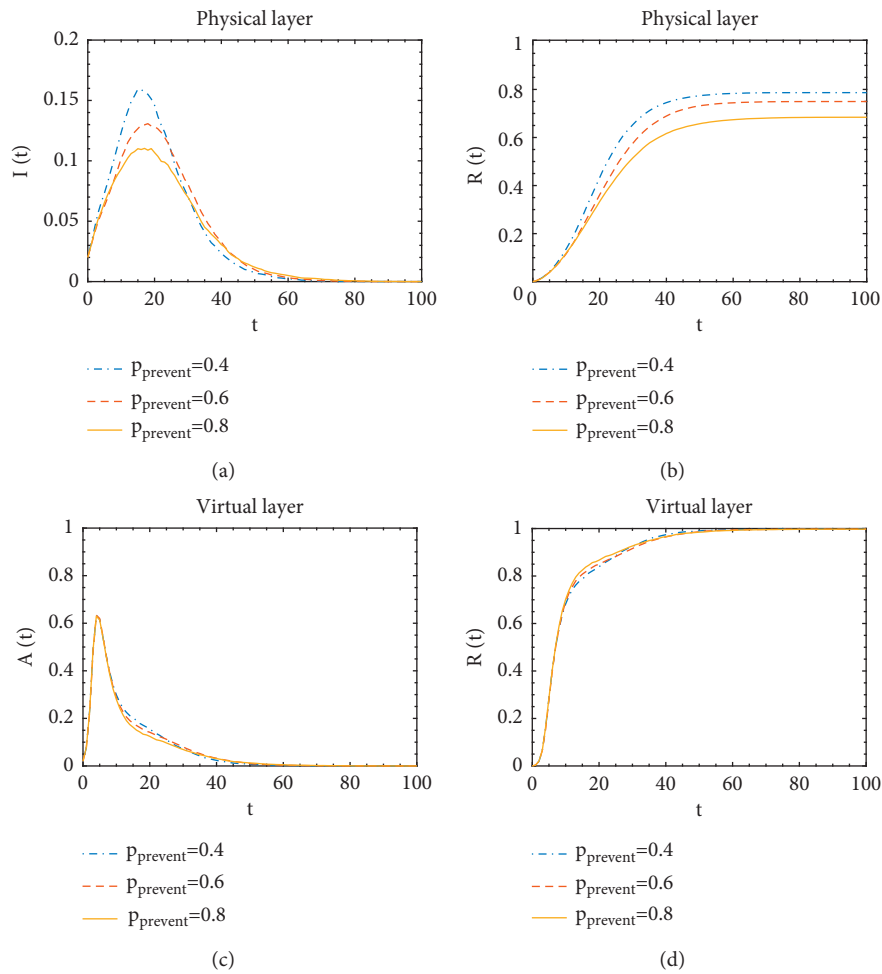


FIGURE 7: Continued.

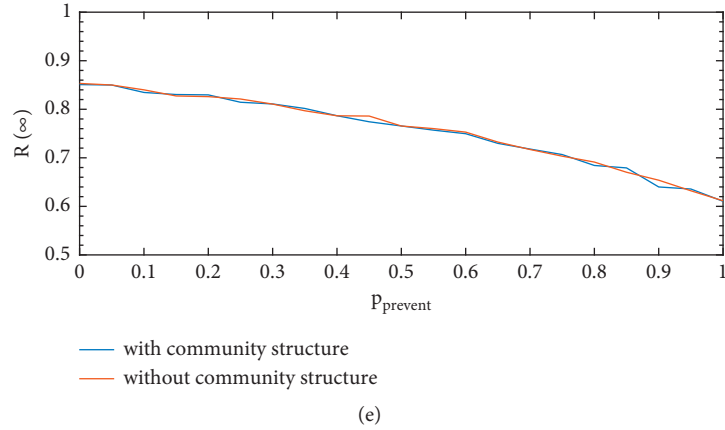


FIGURE 7: The influence of taking preventive behaviors on the coupled disease-awareness model. (a) Density of infected individuals in the physical layer as a function of time. (b) Density of recovered individuals in the physical layer as a function of time. (c) Density of aware individuals in the virtual layer as a function of time. (d) Density of recovered individuals in the virtual layer as a function of time. (e) The final density of recovered individuals in the physical layer under different probabilities of taking preventive behaviors for the virtual contact networks with or without community structure.

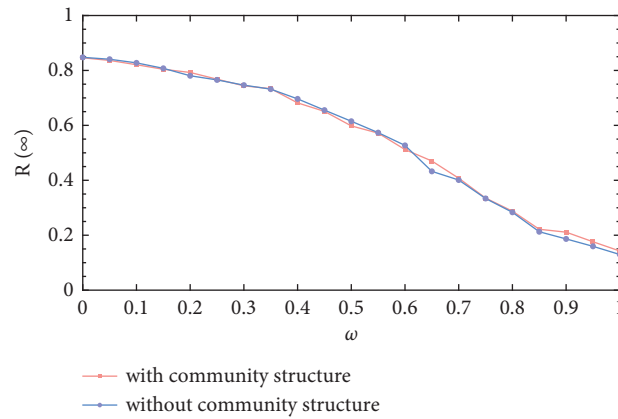


FIGURE 8: The final density of recovered individuals in the physical layer under different parameters ω for the virtual contact networks with or without community structure.

We investigate the impact of the parameter ω on the disease transmission, and the result is shown in Figure 8. We fixed the following parameters: $\beta_1 = 0.2$, $\beta_2 = 0.3$, $p_{\text{jump}} = 0.2$, $p_{\text{prevent}} = 0.8$. The results in the two scenarios—virtual contact network with or without community structure—are similar. We can find that the stronger the effect of taking protective actions, the smaller the scale of disease transmission. When the parameter $\omega \in [0, 0.35]$, the final density of recovered individuals in the physical layer slowly decreases as ω increases. But when the parameter ω is greater than 0.35, the final density of recovered individuals in the physical layer will decrease rapidly as ω increases.

Finally, we analyze the impact of changing long-distance jump probability p_{jump} on the spread of disease and information shown in Figure 9. We fixed the following parameters: $\beta_1 = 0.2$, $\beta_2 = 0.3$, $p_{\text{prevent}} = 0.8$. In Figure 9(a), we can find that increasing the value of p_{jump} can increase the peak value of the density of infected individuals. The

evolution processes of information dissemination with $p_{\text{jump}} = 0.4$ is closer to the performance of $p_{\text{jump}} = 0.6$, but it is quite different from the results of $p_{\text{jump}} = 0.2$. When the parameter p_{jump} is increased from 0.2 to 0.6, the peak value of the density of infected individuals rises. We observe that the final density of recovered individuals in the physical layer increases as p_{jump} increases in Figure 9(b). Infected individuals accelerate the global spread of the disease through long-distance jumping. We also see that the peak value of the density of aware individuals and the final density of recovered individuals in the virtual layer increase as the parameter p_{jump} increases in Figures 9(c) and 9(d), but this growth trend is not very obvious. In addition, in Figure 9(e), we also investigate the final density of the recovered individuals in the physical layer under different probabilities p_{jump} . We can observe that the increase of p_{jump} can accelerate the spread of disease. But when the parameter p_{jump} is greater than 0.4, the final density of recovered individuals in the virtual layer basically remains stable.

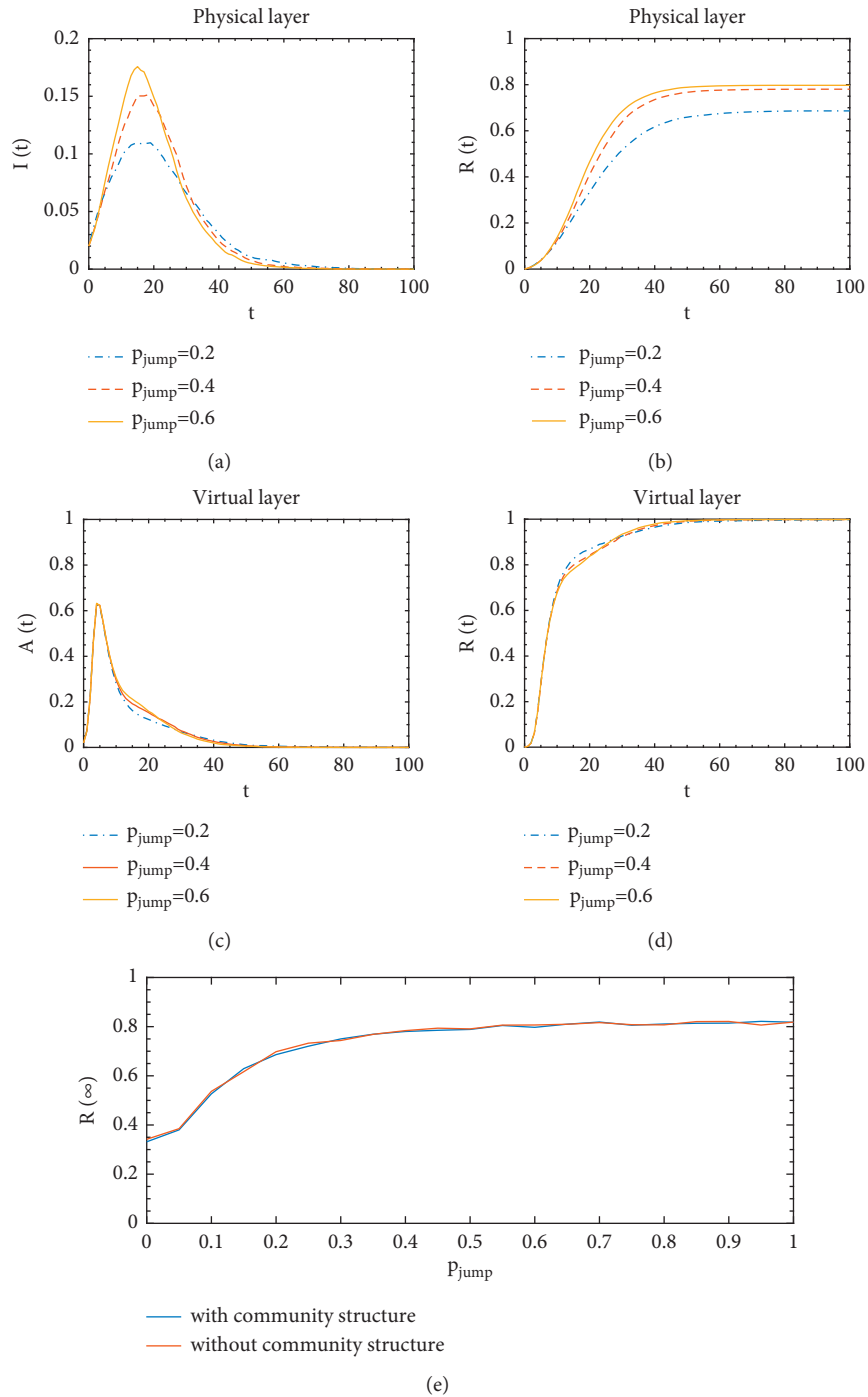


FIGURE 9: The influence of long-distance jump on the coupled disease-awareness model. (a) Density of infected individuals in the physical layer as a function of time. (b) Density of recovered individuals in the physical layer as a function of time. (c) Density of aware individuals in the virtual layer as a function of time. (d) Density of recovered individuals in the virtual layer as a function of time. (e) The final density of recovered individuals in the physical layer under different probabilities of jumping for the virtual contact networks with or without community structure.

4. Conclusions

Based on the idea that the network structure can have a significant impact on network dynamics, in this article, we investigate how a multiplex virtual-physical contact network with a community structure affects the spread of diseases

and information. The multiplex network we built contains two layers: virtual layer and physical layer. We assume that the virtual layer is a static communication network with a community structure and the physical layer is a dynamic physical contact network, which contains individuals. In our model, we assume that the individuals often choose to move

in a fixed area, and they move across regions with a small probability through a long-distance jump. It indicates that in the physical contact network, nodes belonging to the same area have more edges, whereas nodes belonging to different areas have fewer edges. Therefore, the physical contact network we built actually has a community structure. When the multiplex virtual-physical contact network has been constructed, we simulate the spread of diseases and information on this multiplex network based on the SIR model and analyze the factors affecting the coupled spreading dynamics. The simulation results show that in this multiplex network with a community structure, promoting the information dissemination can inhibit the epidemic spreading, but changing the epidemic spreading has no obvious impact on information dissemination. We find that increasing the information transmission rate or the probability of taking preventive behaviors and decreasing the long-distance jump probability can reduce the peak value of the density of infected individuals. Compared with information transmission rate, we also observe that the effect of taking preventive behaviors or decreasing the long-distance jump on suppressing the spread of disease is more obvious. However, changing the epidemic transmission rate does not significantly affect the information dissemination. By comparing the simulation results under the two scenarios—virtual layer with or without community structure—the community structure of virtual contact network has no significant impact on disease transmission. This research deepens our understanding of the interaction between disease transmission and information transmission.

Through this research, we realize that taking preventive behaviors or decreasing the long-distance jump has a significant impact on the control epidemic spreading. Therefore, in reality we should raise awareness of prevention and minimize unnecessary trips. Considering that promoting the dissemination of information about the disease can slow down the spread of the disease; therefore, when an epidemic breaks out, we should use various platforms to promote information dissemination. Although this article has analyzed the factors affecting the evolution of coupling dynamics, we still do not know the relationship between these factors and the epidemic outbreak threshold. In the future, we will try to use theoretical analysis to explain how other factors affect the epidemic outbreak threshold.

Data Availability

The data used to support the findings of this study are available from the corresponding author upon request.

Conflicts of Interest

The authors declare that they have no conflicts of interest.

Acknowledgments

This work was supported by the National Natural Science Foundation of China (Grant no. 71673256).

References

- [1] S. Funk, M. Salathé, and V. A. A. Jansen, “Modelling the influence of human behaviour on the spread of infectious diseases: a review,” *Journal of The Royal Society Interface*, vol. 7, no. 50, pp. 1247–1256, 2010.
- [2] Z. Wang, M. A. Andrews, Z.-X. Wu, L. Wang, and C. T. Bauch, “Coupled disease-behavior dynamics on complex networks: a review,” *Physics of Life Reviews*, vol. 15, pp. 1–29, 2015.
- [3] W. Wang, Q.-H. Liu, J. Liang, Y. Hu, and T. Zhou, “Co-evolution spreading in complex networks,” *Physics Reports*, vol. 820, pp. 1–51, 2019.
- [4] S. Funk, E. Gilad, C. Watkins, and V. A. A. Jansen, “The spread of awareness and its impact on epidemic outbreaks,” *Proceedings of the National Academy of Sciences*, vol. 106, no. 16, pp. 6872–6877, 2009.
- [5] C. T. Bauch and A. P. Galvani, “Social factors in epidemiology,” *Science*, vol. 342, no. 6154, pp. 47–49, 2013.
- [6] W. Wang, M. Tang, H. Yang, Y. Younghae Do, Y. C. Lai, and G. Lee, “Asymmetrically interacting spreading dynamics on complex layered networks,” *Scientific Reports*, vol. 4, p. 5097, 2014.
- [7] H. Wang, C. Ma, H. S. Chen, and H. F. Zhang, “Effects of asymptomatic infection and self-initiated awareness on the coupled disease-awareness dynamics in multiplex networks,” *Applied Mathematics and Computation*, vol. 400, Article ID 126084, 2021.
- [8] W. Duan, Z. Fan, P. Zhang, G. Guo, and X. Qiu, “Mathematical and computational approaches to epidemic modeling: a comprehensive review,” *Frontiers of Computer Science*, vol. 9, no. 5, pp. 806–826, 2015.
- [9] R. Pastor-Satorras, C. Castellano, P. Van Mieghem, and A. Vespignani, “Epidemic processes in complex networks,” *Reviews of Modern Physics*, vol. 87, no. 3, pp. 925–979, 2015.
- [10] R. Pastor-Satorras and A. Vespignani, “Epidemic spreading in scale-free networks,” *Physical Review Letters*, vol. 86, no. 14, pp. 3200–3203, 2001.
- [11] D. Volchenkov, L. Volchenkova, and P. Blanchard, “Epidemic spreading in a variety of scale free networks,” *Physical review. E, Statistical, nonlinear, and soft matter physics*, vol. 66, no. 4, Article ID 046137, 2002.
- [12] X. Chu, J. Guan, Z. Zhang, and S. Zhou, “Epidemic spreading in weighted scale-free networks with community structure,” *Journal of Statistical Mechanics: Theory and Experiment*, vol. 2009, Article ID P07043, 2009.
- [13] P. Zhu, Q. Zhi, Y. Guo, and Z. Wang, “Analysis of epidemic spreading process in adaptive networks,” *IEEE Transactions on Circuits and Systems II: Express Briefs*, vol. 66, no. 7, pp. 1252–1256, 2019.
- [14] H. Kang, M. Sun, Y. Yu, X. Fu, and B. Bao, “Spreading dynamics of an SEIR model with delay on scale-free networks,” *IEEE Transactions on Network Science and Engineering*, vol. 7, no. 1, pp. 489–496, 2020.
- [15] S. Xu, W. Lu, L. Xu, and Z. Zhan, “Adaptive epidemic dynamics in networks: thresholds and control,” *ACM Transactions on Autonomous and Adaptive Systems*, vol. 8, no. 4, p. 19, 2014.
- [16] S. Funk, E. Gilad, and V. A. A. Jansen, “Endemic disease, awareness, and local behavioural response,” *Journal of Theoretical Biology*, vol. 264, no. 2, pp. 501–509, 2010.
- [17] Z. Ruan, M. Tang, and Z. Liu, “Epidemic spreading with information-driven vaccination,” *Physical review. E*,

- Statistical, nonlinear, and soft matter physics*, vol. 86, no. 3, Article ID 036117, 2012.
- [18] C. Granell, S. Gómez, and A. Arenas, “Dynamical interplay between awareness and epidemic spreading in multiplex networks,” *Physical Review Letters*, vol. 111, no. 12, Article ID 128701, 2013.
- [19] C. Granell, S. Gómez, and A. Arenas, “Competing spreading processes on multiplex networks: awareness and epidemics,” *Physical review. E, Statistical, nonlinear, and soft matter physics*, vol. 90, no. 1, Article ID 012808, 2014.
- [20] M. Salehi, R. Sharma, M. Marzolla, M. Magnani, P. Siyari, and D. Montesi, “Spreading processes in multilayer networks,” *IEEE Transactions on Network Science and Engineering*, vol. 2, no. 2, pp. 65–83, 2015.
- [21] Q. Guo, X. Jiang, Y. Lei, M. Li, Y. Ma, and Z. Zheng, “Two-stage effects of awareness cascade on epidemic spreading in multiplex networks,” *Physical review. E, Statistical, nonlinear, and soft matter physics*, vol. 91, no. 1, Article ID 012822, 2015.
- [22] M. Scata, A. D. Stefano, P. Lio, and A. La Corte, “The impact of heterogeneity and awareness in modeling epidemic spreading on multiplex networks,” *Scientific Reports*, vol. 6, Article ID 37105, 2016.
- [23] J.-Q. Kan and H.-F. Zhang, “Effects of awareness diffusion and self-initiated awareness behavior on epidemic spreading - an approach based on multiplex networks,” *Communications in Nonlinear Science and Numerical Simulation*, vol. 44, pp. 193–203, 2017.
- [24] K. M. A. Kabir and J. Tanimoto, “Analysis of epidemic outbreaks in two-layer networks with different structures for information spreading and disease diffusion,” *Communications in Nonlinear Science and Numerical Simulation*, vol. 72, pp. 565–574, 2019.
- [25] D. Zhao, L. Wang, Z. Wang, and G. Xiao, “Virus propagation and patch distribution in multiplex networks: modeling, analysis, and optimal allocation,” *IEEE Transactions on Information Forensics and Security*, vol. 14, no. 7, pp. 1755–1767, 2019.
- [26] F. D. Sahneh, A. Vajdi, J. Melander, and C. M. Scoglio, “Contact adaption during epidemics: a multilayer network formulation approach,” *IEEE Transactions on Network Science and Engineering*, vol. 6, no. 1, pp. 16–30, 2019.
- [27] C. Xia, Z. Wang, C. Zheng et al., “A new coupled disease-awareness spreading model with mass media on multiplex networks,” *Information Sciences*, vol. 471, pp. 185–200, 2019.
- [28] N. An, H. Chen, C. Ma, and H. Zhang, “Spontaneous symmetry breaking and discontinuous phase transition for spreading dynamics in multiplex networks,” *New Journal of Physics*, vol. 20, no. 12, Article ID 125006, 2018.
- [29] H. Wang, C. Ma, H. Chen, and H. Zhang, “Effect of overlap on spreading dynamics on multiplex networks,” *J. Stat. Mech*, vol. 2020, no. 4, Article ID 043402, 2020.
- [30] L. Xia, B. Song, Z. Jing, Y. Song, and L. Zhang, “Dynamical interaction between information and disease spreading in populations of moving agents,” *Computers, Materials & Continua*, vol. 57, no. 1, pp. 123–144, 2018.
- [31] Y. Yang, H. Liu, and J. Zhou, “Epidemic spreading-information dissemination coupling mechanism in heterogeneous areas,” *Computers, Materials & Continua*, vol. 67, no. 3, pp. 3311–3327, 2021.
- [32] S. Gómez, A. Díaz-Guilera, J. Gómez-Gardeñes, C. J. Pérez-Vicente, Y. Moreno, and A. Arenas, “Diffusion dynamics on multiplex networks,” *Physical Review Letters*, vol. 110, no. 2, Article ID 028701, 2013.
- [33] M. Dickison, S. Havlin, and H. E. Stanley, “Epidemics on interconnected networks,” *Physical review. E, Statistical, nonlinear, and soft matter physics*, vol. 85, no. 6, Article ID 066109, 2012.
- [34] S. Fortunato and D. Hric, “Community detection in networks: a user guide,” *Physics Reports*, vol. 659, pp. 1–44, 2016.
- [35] M. Frasca, A. Buscarino, A. Rizzo, L. Fortuna, and S. Boccaletti, “Dynamical network model of infective mobile agents,” *Physical review. E, Statistical, nonlinear, and soft matter physics*, vol. 74, no. 3, Article ID 036110, 2006.
- [36] A. Buscarino, L. Fortuna, M. Frasca, and V. Latora, “Disease spreading in populations of moving agents,” *Europhysics Letters*, vol. 82, no. 3, Article ID 38002, 2008.
- [37] A. Buscarino, L. Fortuna, M. Frasca, and A. Rizzo, “Local and global epidemic outbreaks in populations moving in inhomogeneous environments,” *Physical review. E, Statistical, nonlinear, and soft matter physics*, vol. 90, no. 4, Article ID 042813, 2014.
- [38] M. E. Newman and M. Girvan, “Finding and evaluating community structure in networks,” *Physical review. E, Statistical, nonlinear, and soft matter physics*, vol. 69, no. 2, Article ID 026113, 2004.